Protection of Toll-Like Receptor 9 Against Lipopolysaccharide-Induced Inflammation and Oxidative Stress of Pulmonary Epithelial Cells via MyD88-Mediated Pathways

Zhenhong QI[1], Jiaxin CHEN[2], Menghua DENG[1], Yunhai ZHANG[1], Tianwei MA[1], Mingyuan MA[1]

[1]Department of Critical Care Medicine, Foshan Hospital of Traditional Chinese Medicine, Foshan, China, [2]Intenal Medicine, The Affiliated Shunde Hospital of Guangzhou Medical University, Foshan, Guangdong, China

Received June 8, 2021
Accepted January 19, 2022
Epub Ahead of Print March 11, 2022

Summary

Acute lung injury (ALI) caused by lipopolysaccharide (LPS) is a common, severe clinical syndrome. Injury caused by inflammation and oxidative stress in vascular endothelial and alveolar epithelial cells is a vital process in the pathogenesis of ALI. Toll-like receptor 9 (TLR9) is highly expressed in LPS-induced ALI rats. In this study, Beas-2B human pulmonary epithelial cells and A549 alveolar epithelial cells were stimulated by LPS, resulting in the upregulation of TLR9 in a concentration-dependent manner. Furthermore, TLR9 overexpression and interference vectors were transfected before LPS administration to explore the role of TLR9 in LPS-induced ALI *in vitro*. The findings revealed that inhibition of TLR9 reduced inflammation and oxidative stress while suppressing apoptosis of LPS-induced Beas-2B and A549 cells, whereas TLR9 overexpression aggravated these conditions. Moreover, TLR9 inhibition resulted in downregulated protein expression of myeloid differentiation protein 88 (MyD88) and activator activator protein 1 (AP-1), as well as phosphorylation of nuclear factor-κB (NF-κB), c-Jun N-terminal kinase (JNK), and p38 mitogen-activated protein kinase (MAPK). The phosphorylation of extracellular-regulated protein kinases 1/2 was upregulated compared to that of cells subjected to only LPS administration, and this was reversed by TLR9 overexpression. These results indicate that inhibition of TLR9 plays a protective role against LPS-induced inflammation and oxidative stress in Beas-2B and A549 cells, possibly via the MyD88/NF-κB and MyD88/MAPKs/AP-1 pathways.

Key words

Acute lung injury • Toll-like receptor 9 • Inflammation • Oxidative stress • MyD88

Corresponding author

Mingyuan Ma, Department of Critical Care Medicine, Foshan Hospital of Traditional Chinese Medicine,Guangdong, Foshan 528000, China. Email: 13500260111@163.com

Introduction

Acute lung injury (ALI) is a complex clinical syndrome induced by many factors, such as inhalation of toxic gases, burns, severe sepsis, severe pneumonia, and severe trauma, resulting in substantial morbidity and mortality [1,2]. Injury caused by inflammation and oxidative stress in vascular endothelial and alveolar epithelial cells is a vital process in the pathogenesis of ALI [2,3]. Although the pathophysiological changes in ALI have been thoroughly studied and treatment methods, such as intensive care and mechanical ventilation, have made great progress, the mortality rate of ALI remains as high as 40 %, exerting a significant impact on public health [2,4]. Lipopolysaccharide (LPS) is an important component of the cell wall of Gram-negative bacteria and can cause ALI by targeting vascular endothelial cells, alveolar epithelial cells, neutrophils, and alveolar macrophages [5]. For this reason, LPS is commonly used to induce and construct ALI models for basic research [6-9].

Toll-like receptors (TLRs) are an important component of the innate immune system and widely distributed in epithelial, endothelial, dendritic, and

immune cells [10]. TLRs are involved in downstream signaling via myeloid differentiation protein 88 (MyD88)-dependent and toll-interleukin 1 receptor domain-containing adapter inducing interferon-β-dependent pathways; these induce the production of interferon (IFN)-stimulated genes and pro-inflammatory cytokines [11]. As one of the subfamilies of TLRs, TLR9 regulates the downstream signaling molecules nuclear factor-κB (NF-κB) and mitogen-activated protein kinases (MAPKs), mainly through the MyD88 signaling pathways, ultimately affecting cellular physiopathological processes [12]. Accumulating evidence has demonstrated that several TLRs, including TLR9, TLR4, and TLR2, are involved in the regulation of ALI, and the effects of TLR4 and TLR2 and their potential mechanisms have been well studied [13-15]. Previous studies have also revealed that TLR9 is highly expressed in rat models of LPS-induced ALI, and inhibition of its expression attenuated the degree of ALI [16]. However, the protective effect of high or low expression of TLR9 on LPS-induced ALI has seldom been reported. In this study, human pulmonary epithelial cells Beas-2B and A549 alveolar epithelial cells were stimulated with LPS to construct a lung injury model to investigate the role of TLR9 *in vitro* through the MyD88 pathway.

Methods

Cell culture and treatment

The Human Pulmonary Epithelial cell line Beas-2B and Elveolar Epithelial cell line A549 were provided by the Shanghai Institutes for Biological Sciences, Chinese Academy of Science (Shanghai, China). After recovery, the cells were grown in RPMI 1640 (Hyclone, Logan, USA) supplemented with 10 % fetal bovine serum (FBS, Gibco, New York, USA), 100 U/ml penicillin (Solarbio, Beijing, China), and 100 μg/ml streptomycin (Solarbio) at 37 °C in a humidified atmosphere containing 5 % CO_2. When the cells reached the logarithmic growth phase, the culture medium was discarded. The cells were washed with phosphate-buffered solution (PBS, Bioswamp, Wuhan, China) and digested with 0.25 % trypsin (Bioswamp, Myhalic Biotechnology Co., Ltd., Wuhan, China) for passaging. The medium was changed every three days.

Cell counting kit-8 (CCK-8) assay

Beas-2B and A549 cells were seeded into 96-well plates at a density of 1×10^3 cells/well. After pretreatment with LPS (Sigma, St. Louis, MO, USA) at 0, 10, 100, 200, 800, or 1000 ng/ml for 24, 48, or 72 h, 10 μl of CCK-8 solution (Bioswamp) was added to each well for 4 h to measure cell viability. A Spectra Max 190 microplate reader (Molecular Devices LLC, Sunnyvale, CA, USA) was used to measure the absorbance at 450 nm. All experiments were performed in triplicates.

LPS preparation method: LPS (1 mg) was resuspended in 1 ml of sterile balanced salt solution or cell culture medium and gently vortexed and shaken until the powder was completely dissolved to obtain 1 mg/ml of storage solution.

Plasmid and transfection

The TLR9 overexpression vector pcDNA3.1 HISA (TLR9 sequence: F: 5'-CGGAATTCCGATGGGTTTCTGCCGCAGC-3', R: 5'-CCCTCGAGGGCTATT-CGGCCGTGGGTCCC-3') and interference vector pSIREN (shRNA1 sequence: 5'-CCTACAACCGCATCGTCAAAC-3', shRNA2 sequence: 5'-GCTGCCCAAATCCCTCATATC-3', shRNA3 sequence: 5'-GCTAGACCTGTCCCACAATAA-3') were purchased from Addgene (Cambridge, MA, USA). Cells (4×10^5 cells/well) were seeded in 24-well plates and cultured until they reached 70-80 % confluence, then transfected with pcDNA3.1-TLR9 (TLR9 overexpression, OV-TLR9), empty pcDNA3.1 HISA vectors (empty TLR9 overexpression vector, OV-TLR9-EV), pSIREN-shTLR9 (TLR9 interference, sh-TLR9), or empty pSIREN vectors (empty TLR9 interference vector, sh-TLR9-EV) using Lipofect-amine2000 (Invitrogen, CA, USA) according to the manufacturer's instructions. Non-transfected Beas-2B and A549 cells were used as controls (CON). After transfection for 24 h, the transfection rate was detected by western blot and the cells were treated with LPS for 24 h. Experiments using each cell type were divided into four groups: LPS (only LPS treatment), LPS+OV-TLR9 (TLR9 overexpression with LPS treatment), LPS+sh-TLR9 (TLR9 interference with LPS treatment), and LPS+EV (TLR9 overexpression empty vector with LPS treatment).

Enzyme-linked immunosorbent assay

After transfection for 24 h, Beas-2B and A549 cells were treated with 100 ng/ml LPS for 24 h, and the expression levels of inflammation-related factors were measured. The levels of interleukin (IL)-6, tumor necrosis factor (TNF)-α, IL-1β, monocyte chemotactic

protein 1 (MCP-1), and monocyte chemotactic protein 5 (MCP-5) in the culture supernatant were detected using ELISA kits (IL-6, HM10205; TNF-α, HM1001; IL-1β; HM10206; MCP-1, HM10894; MCP-5, HM10983; Bioswamp) according to the manufacturer's protocols. The absorbance was measured at 450 nm using a Labsystems Multiskan MS-352 microplate reader (Vantaa, Finland). The levels of inducible nitric oxide synthase (iNOS), endothelial nitric oxide synthase (eNOS), and nitric oxide (NO) were measured according to the instructions of the respective kits designed by Nanjing Jiancheng Bioengineering Institute (iNOS, A014-1; eNOS, H195; NO, A012-1, Nanjing, China). All experiments were performed in triplicates.

Flow cytometry

After transfection for 24 h, Beas-2B and A549 cells were treated with 100 ng/ml LPS for 24 h. Cell apoptosis and reactive oxygen species (ROS) levels were evaluated using flow cytometry (Beckman Coulter, Brea, CA, USA). Cell apoptosis was evaluated using an annexin V-fluorescein isothiocyanate (FITC)/propidium iodide (PI) kit (Bioswamp) according to the manufacturer's protocol. Cells were suspended at a concentration of 1×10^5 cells in 200 µl of binding buffer. Annexin V-FITC and PI (10 µl of each) were added and the cells were incubated for 30 min in the dark, after which the cells were analyzed by flow cytometry. For the ROS level assay, the collected cells (1×10^7/ml) were resuspended in diluted dihydroethidium for 20 min at 37 °C and subjected to flow cytometry.

Western blot assay

Total proteins were extracted from Beas-2B and A549 cells using radioimmunoprecipitation assay lysis buffer (Bioswamp) containing a cocktail of protease and phosphatase inhibitors. Protein concentration was quantified using a bicinchoninic acid kit (Bioswamp). Protein samples (20 µg) were separated by sodium dodecyl sulfate-polyacrylamide gel electrophoresis and transferred onto polyvinylidene fluoride membranes (Millipore, Boston, Massachusetts, USA). The membranes were blocked with 5 % skim milk for 2 h at room temperature then incubated overnight at 4 °C with primary antibodies against TLR9 (Ab37154, 1:1000, Abcam, Cambridge, UK), MyD88 (Ab2064, 1:1000, Abcam), nuclear factor (NF)-κB (Ab16502, 1:2000, Abcam), p-NF-κB (Ab86299, 1:5000, Abcam), activator protein 1 (AP-1, Ab31419, 1:1000, Abcam), extracellular-regulated protein kinases (ERK)1/2 (Ab17942, 1:1000, Abcam), p-ERK1/2 (Ab50011, 1:10000, Abcam), c-Jun N-terminal kinase (JNK, Ab179461, 1:1000, Abcam), p-JNK (Ab124956, 1:5000, Abcam), p38 mitogen-activated protein kinase (MAPK, Ab31828, 1:1000, Abcam), p-p38MAPK (Ab47363, 1:1000, Abcam), caspase 8 (Ab25901, 1:1000, Abcam), Bcl-2 (Ab196495, 1:1000, Abcam), and glyceraldehyde 3-phosphate dehydrogenase (GAPDH; 2118, 1:1000; Cell Signaling Technology, Danvers, MA, USA). After washing with PBS/Tween 20, the membranes were incubated with goat anti-rabbit IgG secondary antibody (PAB160011, 1:10000, Bioswamp) for TLR9 and goat anti-mouse IgG (PAB150009, 1:10000, Bioswamp) for 1 h at room temperature. Immunoreactivity was visualized by a colorimetric reaction using an enhanced chemiluminescence substrate buffer (Millipore, Massachusetts, USA). The membranes were then detected using an automatic chemiluminescence analyzer (Tanon-5200, Shanghai, China), and the relevant band gray values were read using the Tanon Gel Imaging Software. All experiments were performed in triplicate.

Statistical analysis

Data are presented as mean ± standard deviation (SD). One-way analysis of variance (ANOVA) was performed using SPSS software (version 19.0; IBM Corp., Armonk, NY, USA) to compare differences between groups, and the least significant difference (LSD) method was used to detect differences between two pairs. Statistical significance was set at $P<0.05$.

Results

Effect of LPS on Beas-2B and A549 cell survival and TLR9 expression

As shown in Fig. 1A and 1B, LPS exerted similar cytotoxic effects on Beas-2B and A549 cells by reducing cell viability in a concentration-dependent manner. In addition, cell viability decreased with the same concentration of LPS for up to 72 h.

Western blot (Fig. 1C and 1D) analysis demonstrated that LPS increased the protein expression of TLR9 in a concentration- and time-dependent manner in both A549 and Beas-2B cells. These results indicated that LPS induced cell damage and increased the expression of TLR9 in both cell types. Based on these results, the selected concentration of LPS was 100 ng/ml and the selected treatment time was 24 h for subsequent

experiments. Under these conditions, the viability of both Beas-2B and A549 cells was significantly lower than that of the control (0 ng/ml LPS) (P<0.001), and the expression of TLR9 was relatively high.

Detection of TRL9 protein expression after transfection

Western blot analysis was used to evaluate the transfection efficiency (Fig. 2). Both A549 and Beas-2B cells transfected with OV-TLR9 exhibited higher TLR9 expression than those in the CON and OV-TLR9-EV (P<0.001). Transfection with sh-TLR9 resulted in a remarkably lower expression of TLR9 than that of CON and sh-TLR9-EV. The cells transfected with OV-TLR9-EV exhibited no significant difference in the expression of TLR9 compared to cells transfected with sh-TLR9-EV. Hence, OV-TLR9-EV cells were chosen as the comparison group in subsequent experiments (termed LPS+EV).

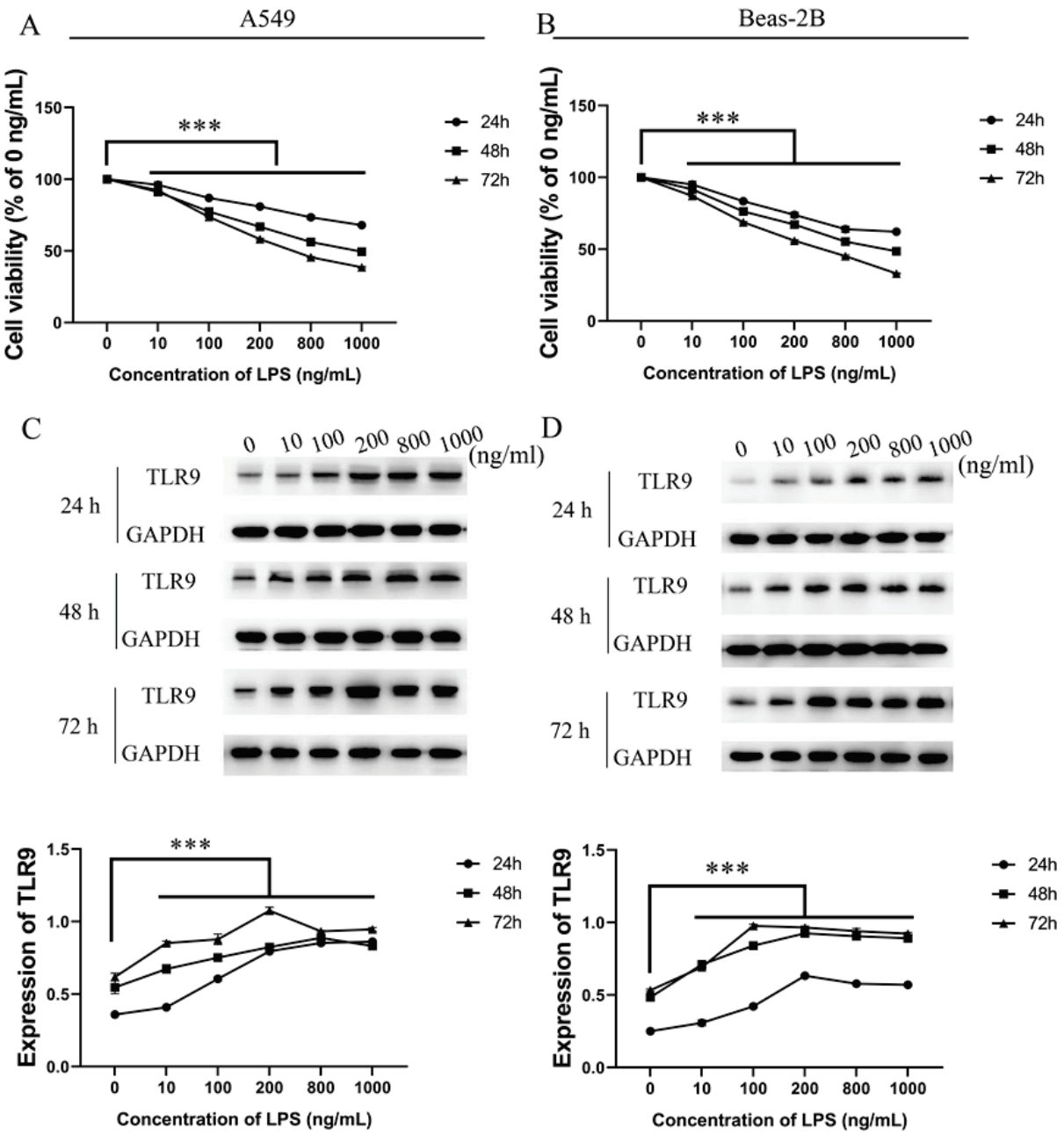

Fig. 1. Effect of LPS on cytotoxicity and TLR9 expression in A549 and Beas-2B cells. The viability of A549 (**A**) and Beas-2B (**B**) cells in response to treatment with different concentrations of LPS at 24, 48, and 72 h. TLR9 protein expression in A549 (**C**) and Beas-2B (**D**) cells in response to treatment with different concentrations of LPS at 24, 48, and 72 h. Data represent mean ± SD (n = 3). ***P<0.001 compared to 0 ng/ml.

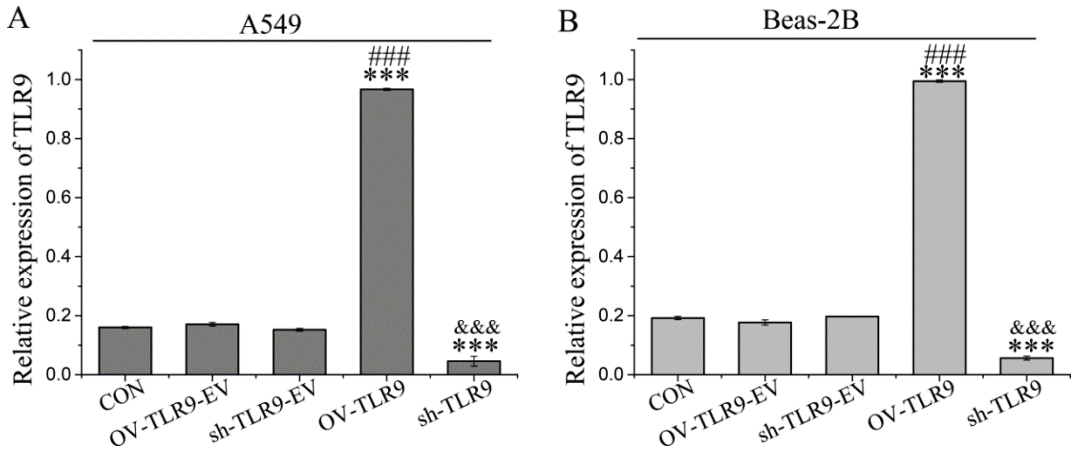

Fig. 2. Detection of TLR9 protein expression after transfection. TLR9 protein expression in A549 (**A**) and Beas-2B (**B**) cells. Data represent mean ± SD (n = 3). ***P < 0.001 compared to CON, $^{###}$P < 0.001 compared to OV-TLR9-EV, $^{\&\&\&}$P < 0.001 compared to sh-TLR9-EV.

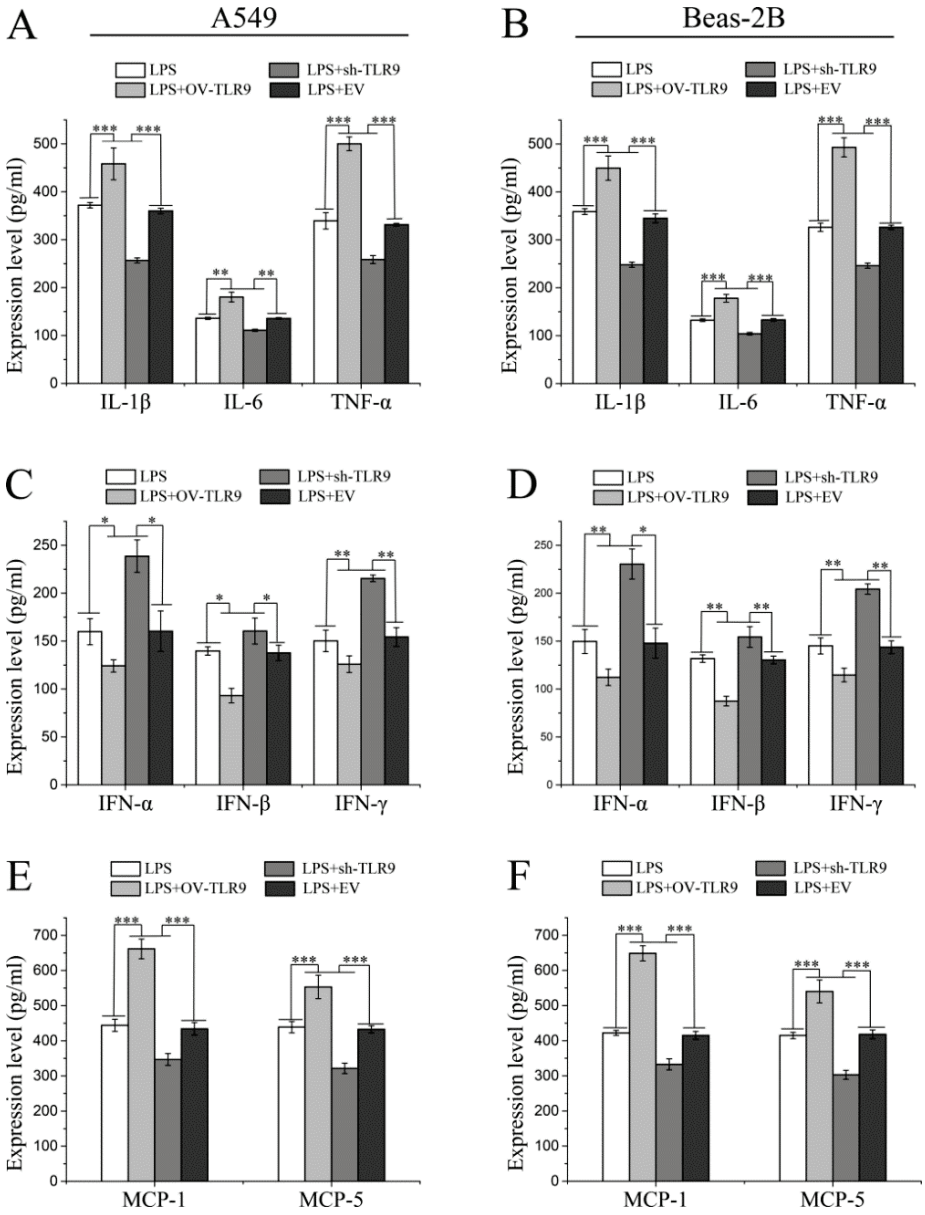

Fig. 3. Effect of TLR9 on the expression of cytokines in supernatants of LPS-challenged A549 and Beas-2B cells. The levels of IL-1β, IL-6, and TNF-α in A549 (**A**) and Beas-2B (**B**) cells. The levels of IFN-γ, IFN-α, and IFN-β in A549 (**C**) and Beas-2B (**D**) cells. The levels of MCP-1 and MCP-5 in A549 (**E**) and Beas-2B (**F**). Data represent mean ± SD (n = 3). *P < 0.05, **P < 0.01, ***P < 0.001

Effect of TLR9 on the expression of inflammation-associated cytokines in LPS-stimulated A549 and Beas-2B cells

Furthermore, the expression levels of inflammation-associated factors IL-1β, IL-6, TNF-α, MCP-1, and MCP-5 in the culture were measured. As shown in Fig. 3A, 3B, 3C, and 3D, both A549 and Beas-2B cells transfected with OV-TLR9 displayed higher expression of IL-1β ($P<0.001$), IL-6 ($P<0.01$), TNF-α ($P<0.001$), MCP-1 ($P<0.001$), and MCP-5 ($P<0.001$) compared to those in the LPS and LPS + EV groups, and transfection with sh-TLR9 displayed remarkably lower expression of these proteins. These results indicated that inhibiting the expression of TLR9 attenuated LPS-induced inflammation, whereas TLR9 overexpression aggravated it.

Effect of TLR9 on oxidative stress in LPS-stimulated A549 and Beas-2B cells

As NO is a vital indicator of oxidative stress, the production of NO and the expression of the related enzymes iNOS and eNOS were detected (Fig. 4). Both Beas-2B and A549 cells transfected with OV-TLR9 exhibited significantly higher expression of iNOS ($P<0.01$) and lower expression of eNOS ($P<0.001$) compared to those of the LPS and LPS + EV groups. Inhibition of TLR9 expression in LPS-stimulated A549 and Beas-2B cells attenuated the levels of iNOS and increased those of eNOS compared to those in the LPS group (Fig. 4A–4D). NO and ROS generation was dramatically increased in the LPS + OV-TLR9 group compared with the LPS group, while transfection with sh-TLR9 markedly reduced NO and ROS production in the LPS group (Fig. 4E, 4F, 4G, and 4H). These results indicated that TLR9 inhibition attenuated LPS-induced oxidative stress, whereas TLR9 overexpression aggravated it.

Effect of TLR9 on LPS-induced apoptosis of A549 and Beas-2B cells

Next, the influence of TLR9 on LPS-induced apoptosis of A549 and Beas-2B cells was assessed. Flow cytometry showed that, compared to the LPS and LPS + EV groups, the percentage of apoptotic cells in the LPS + OV-TLR9 group was higher, whereas that in the LPS + sh-TLR9 group was lower (Fig. 5A and 5B). The expression of the apoptosis-related proteins caspase 8 and

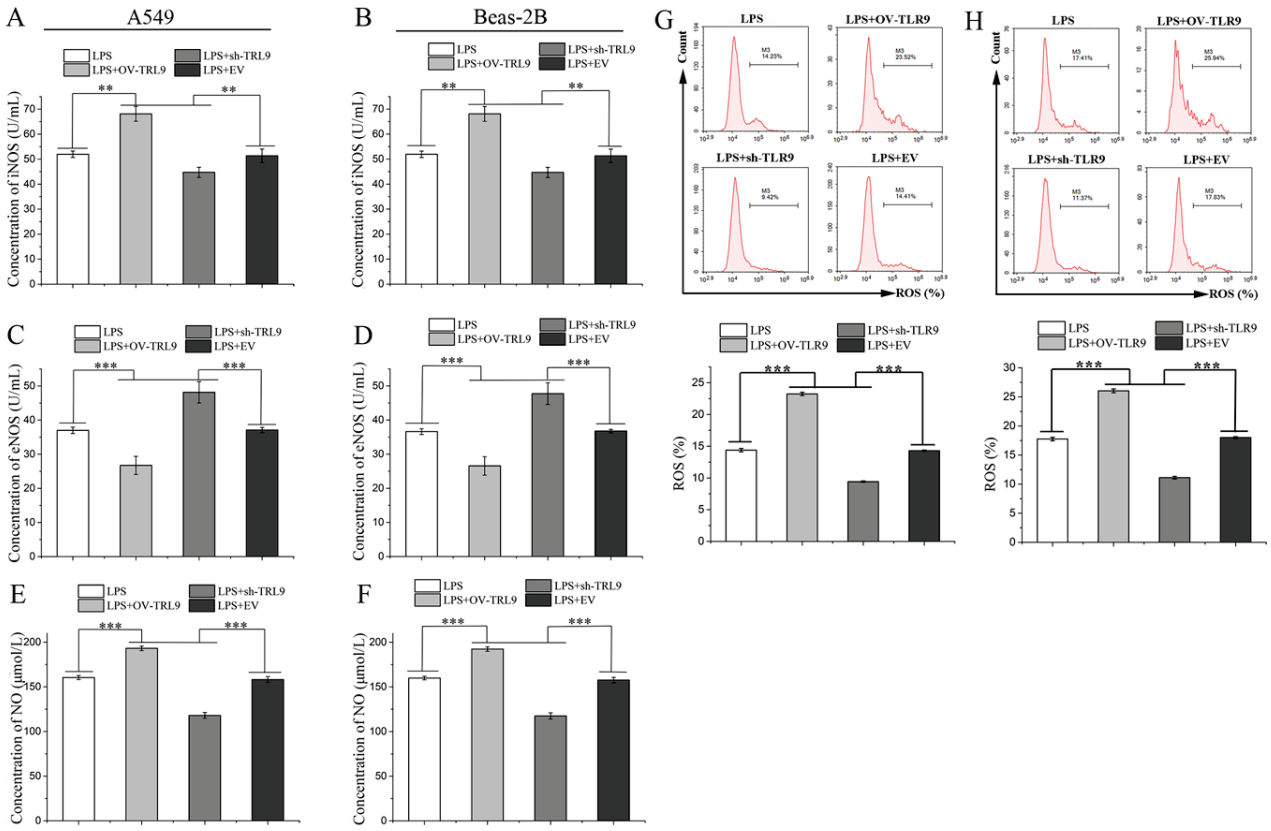

Fig. 4. Effect of TLR9 on iNOS, eNOS, NO, and ROS production in supernatants of LPS-stimulated A549 and Beas-2B cells. iNOS level in A549 (**A**) and Beas-2B (**B**) cells. eNOS level in A549 (**C**) and Beas-2B (**D**) cells. NO generation in A549 (**E**) and Beas-2B (**F**) cells. The ROS level in A549 (**G**) and Beas-2B (**H**) cells. Data represent mean ± SD (n = 3). **P < 0.01, ***P < 0.001.

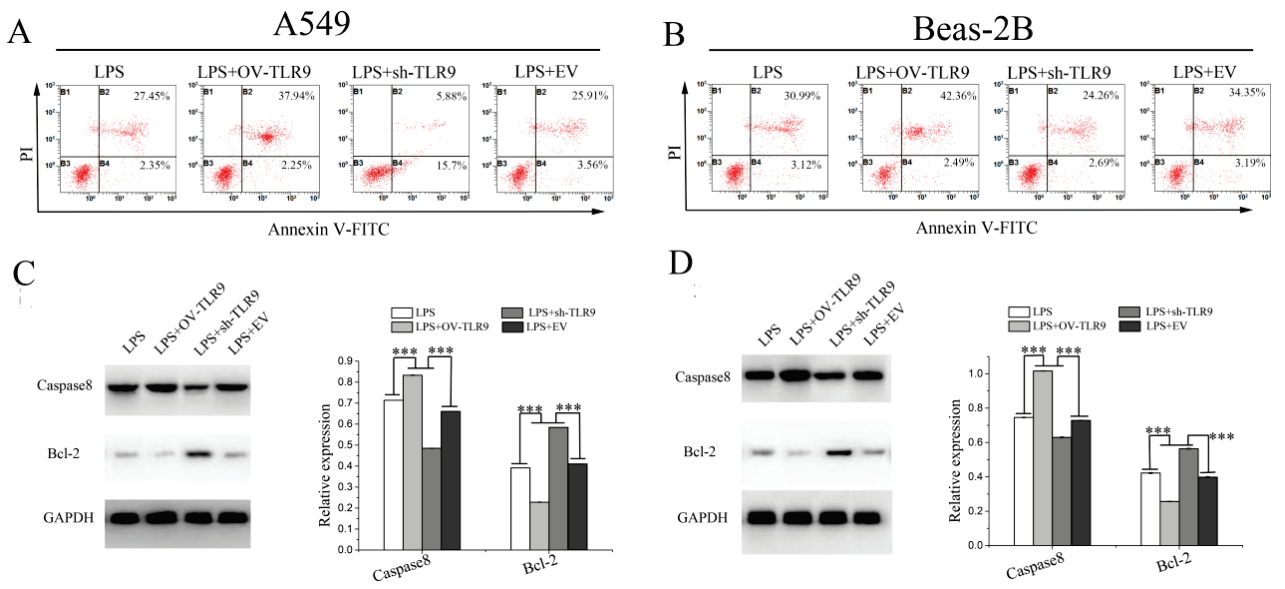

Fig. 5. Effect of TLR9 on LPS-induced apoptosis in A549 and Beas-2B cells. Flow cytometry was used to measure the percentage of apoptotic A549 (**A**) and Beas-2B (**B**) cells. Expression of apoptosis-related proteins caspase 8 and Bcl-2 in A549 (**C**) and Beas-2B (**D**) cells. Data represent mean ± SD (n = 3). ***P < 0.001.

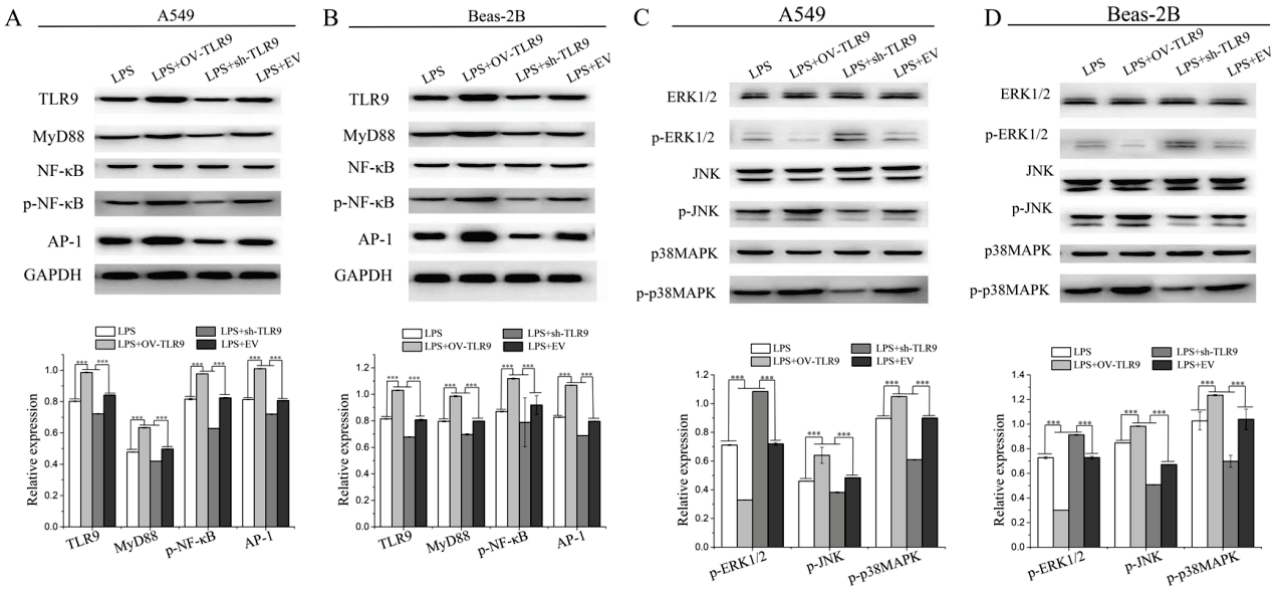

Fig. 6. Effect of TLR9 on the protein expression in LPS-challenged A549 and Beas-2B cells. The protein expression of MyD88, NF-κB, p-NF-κB, and AP-1 in A549 (**A**) and Beas-2B (**B**) cells. The protein expression of p-ERK1/2, p-JNK, and p-p38MAPK in A549 (**C**) and Beas-2B (**D**) cells. Data represent mean ± SD (n = 3). ***P < 0.001.

Bcl-2 was measured by western blotting (Fig. 5C and 5D) and showed the same tendency in A549 and Beas-2B cells. Compared to the LPS and LPS + EV groups, the expression of the pro-apoptotic protein caspase 8 in the LPS + OV-TLR9 group was upregulated (P<0.001) and that in the LPS + sh-TLR9 group was downregulated (P<0.001). The expression of the anti-apoptotic protein Bcl-2 in the LPS + OV-TLR9 group was downregulated (P<0.001) and that in the LPS + sh-TLR9 group was upregulated (P<0.001) compared to that in the LPS and LPS + EV groups. These results indicate that TLR9 promotes LPS-induced apoptosis and that interference of TLR9 expression plays a protective role against apoptosis.

Effect of TLR9 on the expression of proteins associated with the TLR9/MyD88/NF-κB and MyD88/MAPKs pathway in LPS-stimulated A549 and Beas-2B cells

As shown in Fig. 6, the tendency of relative protein expression was similar in A549 and Beas-2B

cells. Cells transfected with OV-TLR9 exhibited higher expression of TLR9, MyD88, p-NF-κB, AP-1, p-JNK, and p-p38MAPK and lower expression of p-ERK1/2 compared to those in the CON and OV-TLR9-EV groups ($P<0.001$). Transfection with sh-TLR9 remarkably lowered the expression of TLR9, MyD88, NF-κB, AP-1, p-JNK, and p-p38MAPK and elevated the expression of p-ERK1/2 compared to those in the CON and sh-TLR9-EV groups ($P<0.001$). These findings implied that the regulation of apoptosis and inflammation by TLR9 in A549 and Beas-2B cells may be mediated by the MyD88 and MAPK signaling pathways.

Discussion

As an important component of the cell wall of Gram-negative bacteria, LPS induces ALI characterized by the overproduction of pro-inflammatory and oxidative stress-related factors. LPS has been extensively applied in the induction and pathogenesis of ALI *in vitro* [17,18]. In the present study, LPS administered to A549 human alveolar epithelial cells and Beas-2B human pulmonary epithelial cells resulted in a remarkable reduction in cell viability and upregulation of TLR9 protein expression. Thus, it was hypothesized that LPS-induced inflammation and oxidative stress in ALI are associated with TLR9 expression. Next, cells were transfected with TLR9 overexpression and interference vectors before LPS treatment to investigate the regulatory effect of TLR9 on LPS-induced inflammation. The results showed that inhibition of TLR9 reduced inflammation and oxidative stress and suppressed LPS-induced apoptosis in A549 and Beas-2B cells, whereas TLR9 overexpression contributed to these processes.

Experimental and clinical research has demonstrated that ALI is an early and deadly complication of septic shock [19]. TLR9 plays an important role in causing hyperinflammation, and its inhibition reduces sepsis-induced mortality by preventing excessive inflammatory responses [20]. Previous studies have shown that TLR9 can be activated by cytosine-phosphate-guanine oligodeoxynucleotides and subsequently recruit MyD88, followed by the activation of downstream NF-κB activation [21]. Activation of the MyD88/NF-κB pathway might result in the release of a large number of inflammatory mediators, such as IL-1β, IL-6, and TNF-α, which aggravate inflammation in the lung and cause ALI [22-24]. Shen *et al*. [10] found that antagonizing or silencing the TLR9 gene attenuated paraquat-induced ALI by suppressing the release of inflammatory cytokines IL-1β and TNF-α mediated by MyD88 and NF-κB, which is consistent with the findings of the present study.

Meanwhile, MyD88 enhances the phosphorylation of MAPKs [25-27], thus regulating the expression of AP-1 and leading to pro-inflammatory cytokine production [28-30]. A large amount of NO is considered an intracellular messenger in the development of oxidative stress [31]. It has been previously demonstrated that reducing iNOS and NO production decreases oxidative stress and cotton smoke-induced lung injury [32]. In recent years, evidence has shown that oxidative stress plays an important role in the development of inflammation [33]. The activation of iNOS induces the prominent production of NO, which causes airway inflammation and tissue damage. It has been reported that iNOS expression is inhibited in response to the downregulation of AP-1 [34], leading to the reduction of NO. However, the production of low concentrations of NO by eNOS protects against excessive bronchoconstriction, and regulates pulmonary blood flow and immune defense. In this study, compared to the LPS group, TLR9 inhibition decreased the levels of iNOS and NO and increased those of eNOS, and these phenomena were reversed by TLR9 overexpression.

AP-1 also regulates the expression of chemokines related to inflammatory responses. Previous research has shown that angiotensin III increases the expression of MCP-1 by activating the transcription factor AP-1, thus promoting the occurrence of cellular inflammation [35]. In addition, MyD88 directly regulates the levels of interferon to influence inflammation [36] and immune responses [37]. In this study, inhibition of TLR9 reduced the levels of the chemokines MCP-1 and MCP-5, while promoting those of IFN-α, IFN-β, and IFN-γ compared to those in the LPS group, and these phenomena were reversed by TLR9 overexpression.

Recent studies have revealed that lung epithelial cell apoptosis is an important pathological feature of LPS-induced ALI [6,17,38]. Arunkumar *et al*. found that TLR9 agonists induced apoptosis in mouse B-cell lymphoma cells by activating NF-κB [39]. The present experimental results indicated that the interference of TLR9 expression attenuated LPS-induced apoptosis in A549 and Beas-2B cells, which was reversed by TLR9 overexpression. The anti-apoptotic protein Bcl-2 is an important member of the Bcl-2 protein family that plays a vital role in the mitochondrial apoptosis pathway [40], while caspase 8 is an important pro-apoptotic protein of the caspase family. In this study, inhibition of TLR9

decreased the protein expression of caspase 8 and increased that of Bcl-2 compared to those in the LPS group, and these phenomena were reversed by TLR9 overexpression, and the trends of each physiological change were consistent in both Beas-2B cells and A549 cells. Yu *et al.* [41] also confirmed the correlation between various physiological changes in both cell types.

In conclusion, our experimental results verified the hypothesis that LPS-induced inflammation and oxidative stress in A549 and Beas-2B cells were associated with TLR9 expression. Inhibition of TLR9 exerted a protective function against LPS-induced inflammation and oxidative stress, which may be relevant to the MyD88/NF-κB and MyD88/MAPK/AP-1 pathways. The present work provides a potential preventive method for the treatment of LPS-induced ALI. Experiments will be performed *in vivo* to further validate these speculations.

Abbreviation

ALI, Acute lung injury; LPS, Lipopolysaccharide; TLR9, Toll-like receptor 9; MyD88, Myeloid differentiation protein 88; AP-1, Activator protein 1; NF-κB, Nuclear factor-κB; JNK, c-Jun N-terminal kinase; MAPK, Mitogen-activated protein kinase; ERK1/2, Extracellular-regulated protein kinases 1/2

Authors' contributions

ZQ and ZH were responsible for the design of this work. ZQ, JC, MM, MD and YZ performed the experiments. ZQ and TM were involved in analyzing data. ZQ drafted the manuscript. ZH revised the manuscript. All authors read and approved the final manuscript.

Conflict of Interest

There is no conflict of interest.

Acknowledgements

This research was mainly hosted by the institute of Sun Yat-sen Memorial Hospital of Sun Yat-sen University, Foshan Hospital of Traditional Chinese Medicine, and Foshan Central Hospital.

References

1. Meng L, Li L, Lu S, Li K, Su Z, Wang Y, Fan X, Li X,Zhao G. The protective effect of dexmedetomidine on LPS-induced acute lung injury through the HMGB1-mediated TLR4/NF-kappaB and PI3K/Akt/mTOR pathways. Mol Immunol 2018; 94: 7-17. https://doi.org/10.1016/j.molimm.2017.12.008
2. Johnson ER, Matthay MA. Acute lung injury: epidemiology, pathogenesis, and treatment. J Aerosol Med Pulm Drug Deliv 2010; 23: 243-252. https://doi.org/10.1089/jamp.2009.0775
3. Mokra D, Kosutova P. Biomarkers in acute lung injury. Respir Physiol Neurobiol 2015; 209: 52-58. https://doi.org/10.1016/j.resp.2014.10.006
4. Maybauer MO, Maybauer DM, Herndon DN. Incidence and outcomes of acute lung injury. N Engl J Med 2006; 354: 416-417.
5. Chen H, Bai C, Wang X. The value of the lipopolysaccharide-induced acute lung injury model in respiratory medicine. Expert Rev Respir Med 2010; 4: 773-783. https://doi.org/10.1586/ers.10.71
6. Gong Y, Lan H, Yu Z, Wang M, Wang S, Chen Y, Rao H, Li J, Sheng Z, Shao J. Blockage of glycolysis by targeting PFKFB3 alleviates sepsis-related acute lung injury via suppressing inflammation and apoptosis of alveolar epithelial cells. Biochemical and biophysical research communications 2017; 491: 522-529. https://doi.org/10.1016/j.bbrc.2017.05.173
7. Yang X, Jing T, Li Y, He Y, Zhang W, Wang B, Xiao Y, Wang W, Zhang J, Wei J, Lin R. Hydroxytyrosol attenuates LPS-induced acute lung injury in mice by regulating autophagy and sirtuin expression. Curr Mol Med 2017; 17: 149-159. https://doi.org/10.2174/1566524017666170421151940
8. Hsieh YH, Deng JS, Pan HP, Liao JC, Huang SS, Huang GJ. Sclareol ameliorate lipopolysaccharide-induced acute lung injury through inhibition of MAPK and induction of HO-1 signaling. Int Immunopharmacol 2017; 44: 16-25. https://doi.org/10.1016/j.intimp.2016.12.026
9. Li Y, Huang J, Foley N M, Xu Y, Li Y P, Pan J, Redmond H P, Wang J H, Wang J. B7H3 ameliorates LPS-induced acute lung injury via attenuation of neutrophil migration and infiltration. Sci Rep 2016; 6: 31284. https://doi.org/10.1038/srep31284

10. Shen H, Wu N, Wang Y, Zhang L, Hu X, Chen Z, Zhao M. Toll-like receptor 9 mediates paraquat-induced acute lung injury: an in vitro and in vivo study. Life Sci 2017; 178: 109-118. https://doi.org/10.1016/j.lfs.2017.03.021
11. Kim A Y, Shim H J, Kim S Y, Heo S, Youn H S. Differential regulation of MyD88- and TRIF-dependent signaling pathways of Toll-like receptors by cardamonin. Int Immunopharmacol 2018; 64: 1-9. https://doi.org/10.1016/j.intimp.2018.08.018
12. Ahmed S, Maratha A, Butt A Q, Shevlin E, Miggin S M. TRIF-mediated TLR3 and TLR4 signaling is negatively regulated by ADAM15. J Immunol 2013; 190: 2217-2228. https://doi.org/10.4049/jimmunol.1201630
13. Cao C, Yin C, Shou S, Wang J, Yu L, Li X, Chai Y. Ulinastatin protects against LPS-induced acute lung injury by attenuating TLR4/NF-kappaB pathway activation and reducing inflammatory mediators. Shock 2018; 50: 595-605. https://doi.org/10.1097/SHK.0000000000001104
14. Feng G, Sun B, Liu H X, Liu Q H, Zhao L, Wang T L. EphA2 antagonism alleviates LPS-induced acute lung injury via Nrf2/HO-1, TLR4/MyD88 and RhoA/ROCK pathways. Int Immunopharmacol 2019; 72: 176-185. https://doi.org/10.1016/j.intimp.2019.04.008
15. Kong D, Wang Z, Tian J, Liu T, Zhou H. Glycyrrhizin inactivates toll-like receptor (TLR) signaling pathway to reduce lipopolysaccharide-induced acute lung injury by inhibiting TLR2. J Cell Physiol 2019; 234: 4597-4607. https://doi.org/10.1002/jcp.27242
16. Han W Z, Xu S W, Wang L. Impact of ketamine intervention for acute lung injury on RAGE and TLR9. Eur Rev Med Pharmacol Sci 2018; 22: 4350-4354. https://doi.org/10.26355/eurrev_201807_15432
17. Shao L, Meng D, Yang F, Song H, Tang D. Irisin-mediated protective effect on LPS-induced acute lung injury via suppressing inflammation and apoptosis of alveolar epithelial cells. Biochemical and biophysical research communications 2017; 487: 194-200. https://doi.org/10.1016/j.bbrc.2017.04.020
18. Zhao J, Yu H, Liu Y, Gibson S A, Yan Z, Xu X, Gaggar A, Li P K, Li C, Wei S, Benveniste E N, Qin H. Protective effect of suppressing STAT3 activity in LPS-induced acute lung injury. Am J Physiol Lung Cell Mol Physiol 2016; 311: L868-L880. https://doi.org/10.1152/ajplung.00281.2016
19. Su CF, Kao S J, Chen HI. Acute respiratory distress syndrome and lung injury: Pathogenetic mechanism and therapeutic implication. World J Crit Care Med 2012; 1: 50-60. https://doi.org/10.5492/wjccm.v1.i2.50
20. Hu D, Yang X, Xiang Y, Li H, Yan H, Zhou J, Caudle Y, Zhang X, Yin D. Inhibition of Toll-like receptor 9 attenuates sepsis-induced mortality through suppressing excessive inflammatory response. Cell Immunol 2015; 295: 92-98. https://doi.org/10.1016/j.cellimm.2015.03.009
21. Knuefermann P, Baumgarten G, Koch A, Schwederski M, Velten M, Ehrentraut H, Mersmann J, Meyer R, Hoeft A, Zacharowski K, Grohe C. CpG oligonucleotide activates Toll-like receptor 9 and causes lung inflammation in vivo. Respir Res 2007; 8: 72. https://doi.org/10.1186/1465-9921-8-72
22. Jiang Q, Yi M, Guo Q, Wang C, Wang H, Meng S, Liu C, Fu Y, Ji H, Chen T. Protective effects of polydatin on lipopolysaccharide-induced acute lung injury through TLR4-MyD88-NF-kappaB pathway. Int Immunopharmacol 2015; 29: 370-376. https://doi.org/10.1016/j.intimp.2015.10.027
23. Herold S, Gabrielli NM, Vadasz I. Novel concepts of acute lung injury and alveolar-capillary barrier dysfunction. Am J Physiol Lung Cell Mol Physiol 2013; 305: L665-681. https://doi.org/10.1152/ajplung.00232.2013
24. Zhao X, Yin L, Fang L, Xu L, Sun P, Xu M, Liu K, Peng J. Protective effects of dioscin against systemic inflammatory response syndromevia adjusting TLR2/MyD88/NFkappab signal pathway. Int Immunopharmacol 2018; 65: 458-469. https://doi.org/10.1016/j.intimp.2018.10.036
25. Yu D, Shi M, Bao J, Yu X, Li Y, Liu W. Genipin ameliorates hypertension-induced renal damage via the angiotensin II-TLR/MyD88/MAPK pathway. Fitoterapia 2016; 112: 244-253. https://doi.org/10.1016/j.fitote.2016.06.010
26. Zong X, Song D, Wang T, Xia X, Hu W, Han F, Wang Y. LFP-20, a porcine lactoferrin peptide, ameliorates LPS-induced inflammation via the MyD88/NF-kappaB and MyD88/MAPK signaling pathways. Dev Comp Immunol 2015; 52: 123-131. https://doi.org/10.1016/j.dci.2015.05.006

27. Zhang R, Ai X, Duan Y, Xue M, He W, Wang C, Xu T, Xu M, Liu B, Li C, Wang Z, Zhang R, Wang G, Tian S, Liu H. Kaempferol ameliorates H9N2 swine influenza virus-induced acute lung injury by inactivation of TLR4/MyD88-mediated NF-kappaB and MAPK signaling pathways. Biomed Pharmacother 2017; 89: 660-672. https://doi.org/10.1016/j.biopha.2017.02.081
28. Gomes M T, Campos P C, Pereira Gde S, Bartholomeu D C, Splitter G, Oliveira S C. TLR9 is required for MAPK/NF-kappaB activation but does not cooperate with TLR2 or TLR6 to induce host resistance to Brucella abortus. J Leukoc Biol 2016; 99: 771-780. https://doi.org/10.1189/jlb.4A0815-346R
29. Cargnello M, Roux PP. Activation and function of the MAPKs and their substrates, the MAPK-activated protein kinases. Microbiol Mol Biol Rev 2011; 75: 50-83. https://doi.org/10.1128/MMBR.00031-10
30. Hossen M J, Kim M Y, Cho J Y. MAPK/AP-1-Targeted Anti-Inflammatory Activities of Xanthium strumarium. Am J Chin Med 2016; 44: 1111-1125. https://doi.org/10.1142/S0192415X16500622
31. Yang Z, Wu QQ, Xiao Y, Duan MX, Liu C, Yuan Y, Meng YY, Liao H H, Tang QZ. Aucubin protects against myocardial infarction-induced cardiac remodeling via nNOS/NO-regulated oxidative stress. Oxid Med Cell Longev 2018; 2018: 4327901. https://doi.org/10.1155/2018/4327901
32. Zhang HX, Liu SJ, Tang XL, Duan GL, Ni X, Zhu XY, Liu YJ, Wang CN. H2S attenuates LPS-induced acute lung injury by reducing oxidative/nitrative stress and inflammation. Cell Physiol Biochem 2016; 40: 1603-1612. https://doi.org/10.1159/000453210
33. Lugrin J, Rosenblatt-Velin N, Parapanov R, Liaudet L. The role of oxidative stress during inflammatory processes. Biol Chem 2014; 395: 203-230. https://doi.org/10.1515/hsz-2013-0241
34. Farombi EO, Shrotriya S, Surh YJ. Kolaviron inhibits dimethyl nitrosamine-induced liver injury by suppressing COX-2 and iNOS expression via NF-kappaB and AP-1. Life Sci 2009; 84: 149-155. https://doi.org/10.1016/j.lfs.2008.11.012
35. Ruiz-Ortega M, Lorenzo O, Egido J. Angiotensin III increases MCP-1 and activates NF-kappaB and AP-1 in cultured mesangial and mononuclear cells. Kidney Int 2000; 57: 2285-2298. https://doi.org/10.1046/j.1523-1755.2000.00089.x
36. Hokeness-Antonelli KL, Crane MJ, Dragoi A M, Chu W M, Salazar-Mather T P. IFN-alphabeta-mediated inflammatory responses and antiviral defense in liver is TLR9-independent but MyD88-dependent during murine cytomegalovirus infection. J Immunol 2007; 179: 6176-6183.
37. Sporri R, Joller N, Albers U, Hilbi H,Oxenius A. MyD88-dependent IFN-gamma production by NK cells is key for control of Legionella pneumophila infection. J Immunol 2006; 176: 6162-6171.
38. Lin W C, Chen C W, Huang Y W, Chao L, Chao J, Lin Y S, Lin C F. Kallistatin protects against sepsis-related acute lung injury via inhibiting inflammation and apoptosis. Sci Rep 2015; 5: 12463. https://doi.org/10.1038/srep12463
39. Arunkumar N, Liu C, Hang H, Song W. Toll-like receptor agonists induce apoptosis in mouse B-cell lymphoma cells by altering NF-kappaB activation. Cell Mol Immunol 2013; 10: 360-372. https://doi.org/10.1038/cmi.2013.14
40. Martinou JC, Youle RJ. Mitochondria in apoptosis: Bcl-2 family members and mitochondrial dynamics. Dev Cell 2011; 21: 92-101. https://doi.org/10.1016/j.devcel.2011.06.017
41. Yu XF, Wang J, No U, Guo S, Sun H, Tong J, Chen T, Li J. The role of miR-130a-3p and SPOCK1 in tobacco exposed bronchial epithelial BEAS-2B transformed cells: Comparison to A549 and H1299 lung cancer cell lines. J Toxicol Environ Health A 2019; 82: 862-869. https://doi.org/10.1080/15287394.2019.1664479

Supplementary material

Table S1. Results of replicate experiments for Biochemical testing in A549 cells

	iNOS (U/ml)	eNOS (U/ml)	NO (μmol/L)
LPS+OV-TLR9	67.40	25.52	195.11
	71.36	24.87	190.30
	65.58	29.77	193.91
LPS	51.78	37.99	158.73
	53.30	36.15	162.88
	50.77	36.90	159.47
LPS+EV	54.22	37.44	161.48
	50.92	36.23	155.02
	48.86	37.63	157.98
LPS+sh-TLR9	45.55	45.55	121.46
	42.40	47.29	117.48
	46.21	51.64	115.06

Table S2. Results of replicate experiments for Biochemical testing in Beas-2B cells

	iNOS (U/ml)	eNOS (U/ml)	NO (μmol/l)
LPS+OV-TLR9	67.37	25.19	194.37
	71.32	24.83	189.52
	65.54	29.68	193.16
LPS	51.73	37.52	158.35
	53.29	35.81	162.16
	50.75	36.55	159.23
LPS+EV	54.19	36.95	160.82
	50.91	36.21	154.76
	48.85	37.19	157.33
LPS+sh-TLR9	45.51	45.18	121.39
	42.37	46.75	116.75
	46.19	51.29	114.37

Table S3. Results of replicate experiments for IL-1β, IL-6, and TNF-α in A549 cells

	TNF-α (pg/ml)		IL-1β (pg/ml)		IL-6 (pg/ml)	
	OD values	**concentration**	**OD values**	**concentration**	**OD values**	**concentration**
LPS+OV-TLR9	1.374	511.302	1.159	433.437	1.274	191.930
	1.312	483.977	1.303	495.791	1.185	176.515
	1.360	505.101	1.187	445.438	1.161	172.401
LPS	0.976	342.031	0.998	365.591	0.959	138.493
	0.924	320.989	1.018	373.912	0.930	133.731
	1.008	355.103	1.023	375.997	0.942	135.698
LPS+EV	0.943	328.649	0.969	353.580	0.948	136.683
	0.949	331.074	0.996	364.761	0.931	133.894
	0.957	334.314	0.989	361.857	0.951	137.177
LPS+sh-TLR9	0.741	248.913	0.731	257.427	0.799	112.548
	0.779	263.627	0.715	251.117	0.775	108.725
	0.778	263.238	0.742	261.776	0.797	112.228

Table S4. Results of replicate experiments for IL-1β, IL-6, and TNF-α in Beas-2B cells

	TNF-α (pg/ml)		IL-1β (pg/ml)		IL-6 (pg/ml)	
	OD values	**concentration**	**OD values**	**concentration**	**OD values**	**concentration**
LPS+OV-TLR9	1.370	509.528	1.147	428.312	1.248	187.401
	1.282	470.881	1.261	477.441	1.174	174.627
	1.345	498.477	1.182	443.290	1.159	172.059
LPS	0.933	324.613	0.967	352.754	0.922	132.421
	0.918	318.577	0.996	364.761	0.906	129.809
	0.961	335.936	0.983	359.371	0.939	135.206
LPS+EV	0.926	321.794	0.926	335.889	0.942	135.698
	0.937	326.226	0.949	345.334	0.926	133.076
	0.949	331.074	0.971	354.407	0.908	130.135
LPS+sh-TLR9	0.722	241.606	0.721	253.481	0.747	104.289
	0.749	252.000	0.694	242.866	0.729	101.450
	0.731	245.063	0.708	248.363	0.762	106.663

Table S5. Results of replicate experiments for IFN-γ, IFN-α, and IFN-β in A549 cells

	IFN-γ (pg/ml)		IFN-α (pg/ml)		IFN-β (pg/ml)	
	OD values	**concentration**	**OD values**	**concentration**	**OD values**	**concentration**
LPS+OV-TLR9	0.517	135.817	0.409	130.261	0.443	84.712
	0.462	119.662	0.394	124.756	0.490	95.250
	0.471	122.293	0.374	117.442	0.508	99.311
LPS	0.554	146.790	0.475	154.683	0.694	142.095
	0.535	141.144	0.461	149.475	0.694	142.095
	0.607	162.656	0.530	175.285	0.662	134.628
LPS+EV	0.567	150.665	0.555	184.724	0.714	146.785
	0.554	146.790	0.461	149.475	0.662	134.628
	0.616	165.367	0.454	146.876	0.648	131.375
LPS+sh-TLR9	0.792	219.401	0.742	256.825	0.823	172.646
	0.771	212.853	0.688	235.734	0.710	145.845
	0.775	214.098	0.656	223.340	0.782	162.858

Table S6. Results of replicate experiments for IFN-γ, IFN-α, and IFN-β in Beas-2B cells

	IFN-γ (pg/ml)		IFN-α (pg/ml)		IFN-β (pg/ml)	
	OD values	**concentration**	**OD values**	**concentration**	**OD values**	**concentration**
LPS+OV-TLR9	0.473	122.878	0.384	121.095	0.431	82.036
	0.433	111.220	0.337	103.992	0.476	92.101
	0.429	110.060	0.358	111.613	0.458	88.064
LPS	0.552	146.195	0.462	149.846	0.669	136.258
	0.518	136.112	0.427	136.889	0.638	129.057
	0.574	152.756	0.495	162.148	0.643	130.215
LPS+EV	0.526	138.478	0.503	165.143	0.662	134.628
	0.535	141.144	0.421	134.677	0.628	126.743
	0.569	151.263	0.446	143.911	0.641	129.752
LPS+sh-TLR9	0.761	209.744	0.716	246.643	0.793	165.477
	0.726	198.913	0.672	229.527	0.702	143.969
	0.743	204.165	0.635	215.248	0.742	153.379

Table S7. Results of replicate experiments for MCP-1 and MCP-5 in A549 cells

	MCP-1 (pg/ml)		MCP-5 (pg/ml)	
	OD values	**concentration**	**OD values**	**concentration**
LPS+OV-TLR9	1.500	693.502	1.172	521.112
	1.415	648.597	1.302	588.202
	1.403	642.303	1.229	550.341
LPS	1.038	456.256	1.040	454.551
	0.973	424.220	0.975	422.352
	1.029	451.801	1.010	439.642
LPS+EV	0.992	433.550	0.976	422.845
	1.030	452.295	0.994	431.725
	0.957	416.385	1.017	443.114
LPS+sh-TLR9	0.789	335.327	0.745	311.483
	0.853	365.945	0.752	314.787
	0.797	339.137	0.802	338.514

Table S8. Results of replicate experiments for MCP-1 and MCP-5 in Beas-2B cells

	MCP-1 (pg/ml)		MCP-5 (pg/ml)	
	OD values	**concentration**	**OD values**	**concentration**
LPS+OV-TLR9	1.457	670.715	1.146	507.877
	1.413	647.547	1.273	573.104
	1.375	627.662	1.208	539.538
LPS	0.979	427.163	0.981	425.308
	0.952	413.940	0.946	408.110
	0.975	425.201	0.952	411.050
LPS+EV	0.948	411.986	0.936	403.216
	0.980	427.654	0.978	423.830
	0.935	405.644	0.983	426.294
LPS+sh-TLR9	0.749	316.354	0.698	289.415
	0.815	347.727	0.731	304.888
	0.786	333.900	0.752	314.787